Shintani M, Yagi H, Nakayama T, Saji T ,Matsuoka R. 2009. A new nonsense mutation of SMAD8 associated with pulmonary arterial hypertension. J Med Genet 46:331-337.

Suzuki H, Hasegawa Y, Kanamaru K ,Zhang JH. 2011a. Mitogen-activated protein kinases in cerebral vasospasm after subarachnoid hemorrhage: a review. Acta Neurochir Suppl 110:133-139.

Suzuki H, Kanamaru K, Shiba M, Fujimoto M, Imanaka-Yoshida K, Yoshida T ,Taki W. 2011b. Cerebrospinal fluid tenascin-C in cerebral vasospasm after aneurysmal subarachnoid hemorrhage. J Neurosurg Anesthesiol 23:310-317.

Suzuki H, Kanamaru K, Suzuki Y, Aimi Y, Matsubara N, Araki T, Takayasu M, Kinoshita N, Imanaka-Yoshida K, Yoshida T ,Taki W. 2010. Tenascin-C is induced in cerebral vasospasm after subarachnoid hemorrhage in rats and humans: a pilot study. Neurol Res 32:179-184.

Suzuki H, Shiba M, Fujimoto M, Kawamura K, Nanpei M, Tekeuchi E, Matsushima S, Kanamaru K, Imanaka-Yoshida K, Yoshida T ,Taki W. 2013. Matricellular protein: a new player in cerebral vasospasm following subarachnoid hemorrhage. Acta Neurochir Suppl 115:213-218.

Trescher K, Thometich B, Demyanets S, Kassal H, Sedivy R, Bittner R, Holzinger C ,Podesser BK. 2013. Type A dissection and chronic dilatation: tenascin-C as a key factor in destabilization of the aortic wall. Interact Cardiovasc Thorac Surg 17:365-370.

Tucker RP , Chiquet-Ehrismann R. 2009. The regulation of tenascin expression by tissue microenvironments. Biochim Biophys Acta 1793:888-892.

Tucker RP, Drabikowski K, Hess JF, Ferralli J, Chiquet-Ehrismann R ,Adams JC. 2006.

Phylogenetic analysis of the tenascin gene family: evidence of origin early in the chordate lineage. BMC Evol Biol 6:60.

Udalova IA, Ruhmann M, Thomson SJ ,Midwood KS. 2011. Expression and immune function of tenascin-C. Crit Rev Immunol 31:115-145.

Van Obberghen-Schilling E, Tucker RP, Saupe F, Gasser I, Cseh B ,Orend G. 2011. Fibronectin and tenascin-C: accomplices in vascular morphogenesis during development and tumor growth. Int J Dev Biol 55:511-525.

Waldo KL, Hutson MR, Ward CC, Zdanowicz M, Stadt HA, Kumiski D, Abu-Issa R ,Kirby ML. 2005. Secondary heart field contributes myocardium and smooth muscle to the arterial pole of the developing heart. Dev Biol 281:78-90.

Wallner K, Li C, Fishbein MC, Shah PK ,Sharifi BG. 1999. Arterialization of human vein grafts is associated with tenascin-C expression. J Am Coll Cardiol 34:871-875.

Wallner K, Shah PK ,Sharifi BG. 2002. Balloon catheterization induces arterial expression of new Tenascin-C isoform. Atherosclerosis 161:75-83.

Wallner K, Sharifi BG, Shah PK, Noguchi S, DeLeon H ,Wilcox JN. 2001. Adventitial remodeling after angioplasty is associated with expression of tenascin mRNA by adventitial myofibroblasts. J Am Coll Cardiol 37:655-661.

Wang L, Shah PK, Wang W, Song L, Yang M ,Sharifi BG. 2013. Tenascin-C deficiency in apo E-/- mouse increases eotaxin levels: implications for atherosclerosis. Atherosclerosis 227:267-274.

Wang L, Wang W, Shah PK, Song L, Yang M ,Sharifi BG. 2012. Deletion of tenascin-C gene exacerbates atherosclerosis and induces intraplaque hemorrhage in Apo-E-deficient mice. Cardiovasc Pathol 21:398-413.

Wang M, Ihida-Stansbury K, Kothapalli D, Tamby MC, Yu Z, Chen L, Grant G, Cheng Y, Lawson JA, Assoian RK, Jones PL ,Fitzgerald GA. 2011. Microsomal prostaglandin e2 synthase-1 modulates the response to vascular injury. Circulation 123:631-639.

Wasteson P, Johansson BR, Jukkola T, Breuer S, Akyurek LM, Partanen J ,Lindahl P. 2008. Developmental origin of smooth muscle cells in the descending aorta in mice. Development 135:1823-1832.

Watanabe G, Nishimori H, Irifune H, Sasaki Y, Ishida S, Zembutsu H, Tanaka T, Kawaguchi S, Wada T, Hata J, Kusakabe M, Yoshida K, Nakamura Y ,Tokino T. 2003. Induction of tenascin-C by tumor-specific EWS-ETS fusion genes. Genes Chromosomes Cancer 36:224-232.

Webb CM, Zaman G, Mosley JR, Tucker RP, Lanyon LE ,Mackie EJ. 1997. Expression of tenascin-C in bones responding to mechanical load. J Bone Miner Res 12:52-58.

Wenk MB, Midwood KS ,Schwarzbauer JE. 2000. Tenascin-C suppresses Rho activation. J Cell Biol 150:913-920.

Wiegreffe C, Christ B, Huang R ,Scaal M. 2009. Remodeling of aortic smooth muscle during avian embryonic development. Dev Dyn 238:624-631.

Xie C, Ritchie RP, Huang H, Zhang J ,Chen YE. 2011. Smooth muscle cell differentiation in vitro: models and underlying molecular mechanisms. Arterioscler Thromb Vasc Biol 31:1485-1494.

Xie WB, Li Z, Shi N, Guo X, Tang J, Ju W, Han J, Liu T, Bottinger EP, Chai Y, Jose PA ,Chen SY. 2013. Smad2 and myocardin-related transcription factor B cooperatively regulate vascular smooth muscle differentiation from neural crest

cells. Circ Res 113:e76-86.

Yamamoto K, Onoda K, Sawada Y, Fujinaga K, Imanaka-Yoshida K, Shimpo H, Yoshida T ,Yada I. 2005. Tenascin-C is an essential factor for neointimal hyperplasia after aortotomy in mice. Cardiovasc Res 65:737-742.

Yamamoto K, Onoda K, Sawada Y, Fujinaga K, Imanaka-Yoshida K, Yoshida T ,Shimpo H. 2007. Locally applied cilostazol suppresses neointimal hyperplasia and medial thickening in a vein graft model. Ann Thorac Cardiovasc Surg 13:322-330.

Yoshimura K , Aoki H. 2012. Recent advances in pharmacotherapy development for abdominal aortic aneurysm. Int J Vasc Med 2012:648167.

Figure Legends

Fig. 1

The modular structure of tenascin-C and known binding receptors.

Each tenascin-C monomer comprises four distinct domains: an assembly domain, EGF-L, constant (grey) and alternatively spliced (black) FNIII repeats, and the C-terminal FBG.(Modified from Midwood et al. , 2011)

Fig. 2

Schematic presentation of the molecular pathway of the mechano-induction of tenascin-C.

Mechanical strain activates RhoA in fibroblasts, depending on fibroncetin, integrin β1 and integrin-linked kinase (ILK), which causes the reduction of monomeric G-actin by inducing actin assembly and stress fiber formation. Depletion of the G-actin pool frees MAL/myocardin-related transcription factor-A (MRTF-A)/ megakaryoblastic leukemia-1 (MKL1) to enter the nucleus, which induces tenascin-C (TNC) expression partly depending on serum response factor (SRF). Meanwhile, TNC interferes with fibronectin-mediated RhoA activation, and finally suppresses TNC transcription. (Adapted from Asparuhova et al., 2009)

Fig. 3

The heterogeneous origin of vascular smooth muscle cells of the aorta and coronary arteries. Different colors explains different embryonic origins for vascular smooth

muscle cells as indicated in the boxed images to the left and right columns. Cardiac neural crest cells form the ascending and aortic arch and branch walls, and preotic neural crest cells contribute to the septal branch coronary artery. The proepicardium, splanchnic mesoderm, and mesothelium are marked by arrows in each boxed image. The mesothelium forms vascular smooth muscle cells of the developing intestine and lung. The yellow line shows that various sources of stem cells contribute to both local and systemic vascular wall.

a, atrium; ao, dorsal aorta; sm, somite; v, ventricle (Adapted from Majesky, 2007)

Fig. 4

Expression pattern of tenascin-C during development of the aorta

(A) Ascending and arch portions of the aorta of whole-mount *lacZ* staining of TNC-reporter mouse embryos at ED12 and 13. (B) Whole mount *lacZ* staining and histological sections of descending portion of the thoracic aorta at ED13-15, immunostained with anti-αSMA(green) and anti-TNC (red). Expression of TNC in medial smooth muscle cells of the aorta is upregulated after ED14-15. Deposition of TNC(red) is detected around lac-Z(blue) /αSMA(green) positive smooth muscle cells in the medial layer. Bar, 50μm

ao, aorta; lpa, left pulmonary artery ; lv, left ventricle; pt, pulmonary trunkt; rv, right ventricle ; TNC, tenascin-C

Fig. 5

Expression pattern of tenascin-C during development of the coronary artery.

(A) Whole mount double immunostaining of a quail heart at ED9. TNC is localized along the αSMA(green) positive coronary artery (arrowheads), Bar, 200μm

(B) Histological section of aorta and coronary artery of a chick embryo at ED10 doubly immunostained with anti-αSMA(green) and anti-TNC(red). For more detail, see Ando et al. 2011. Bar, 50μm, ao, aorta; av, aortic valve; co, coronary artery; pt, pulmonary trunk; TNC, tenascin-C; αSMA, α-smooth muscle actin

Fig. 6

Crosstalk signaling between tenascin-C/integrin αvβ3 and PDGF-BB/PDGFR-β in vascular smooth muscle cells. TNC facilitates PDGFR recruitment to focal adhesion complex and arguments PDGF signaling by cross-talk between PDGFR-β and integrin αvβ3, being accompanied by phosphorylation of focal adhesion kinase (FAK) and Src tyrosine kinase(SRC). These finally enhances cell proliferation by ERK activation, and migration by RhoA inhibition and activation of PI3K, RAC and myosin light chain kinase(MLCK).

Fig.1

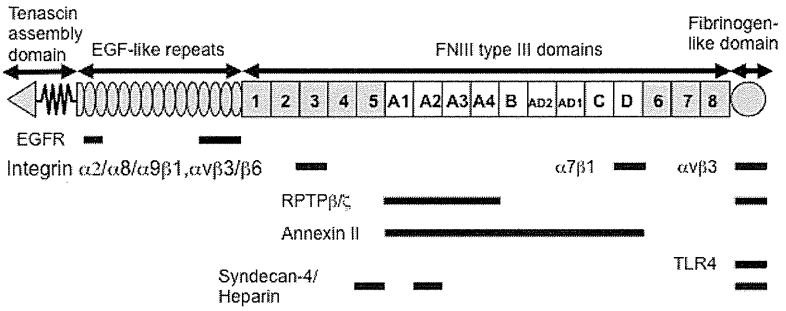
Tenascin assembly domain
EGF-like repeats
FNIII type III domains
Fibrinogen-like domain
1
2
3
4
5
A1
A2
A3
A4
B
AD2
AD1
C
D
6
7
8
EGFR
Integrin α2/α8/α9β1,αvβ3/β6
α7β1
αvβ3
RPTPβ/ζ
Annexin II
TLR4
Syndecan-4/ Heparin

Fig.2

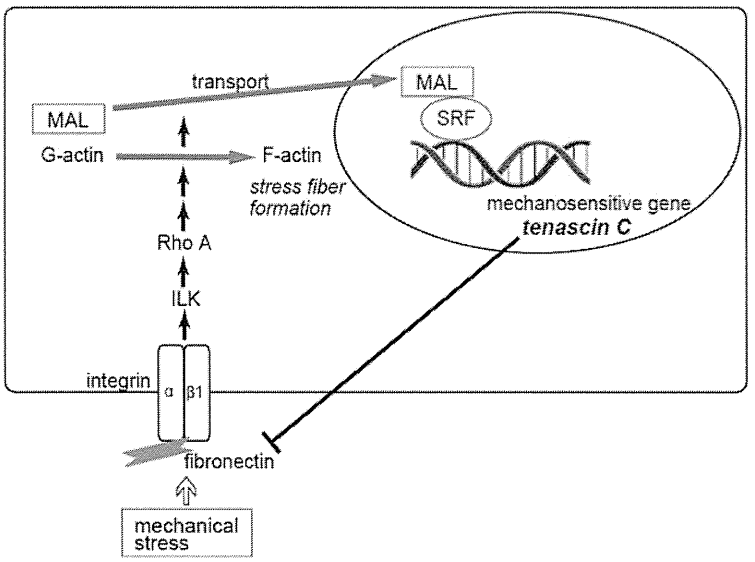
transport
MAL
MAL
SRF
G-actin
F-actin
stress fiber
formation
mechanosensitive gene
tenascin C
Rho A
ILK
integrin
α
β1
fibronectin
mechanical
stress

Fig.3

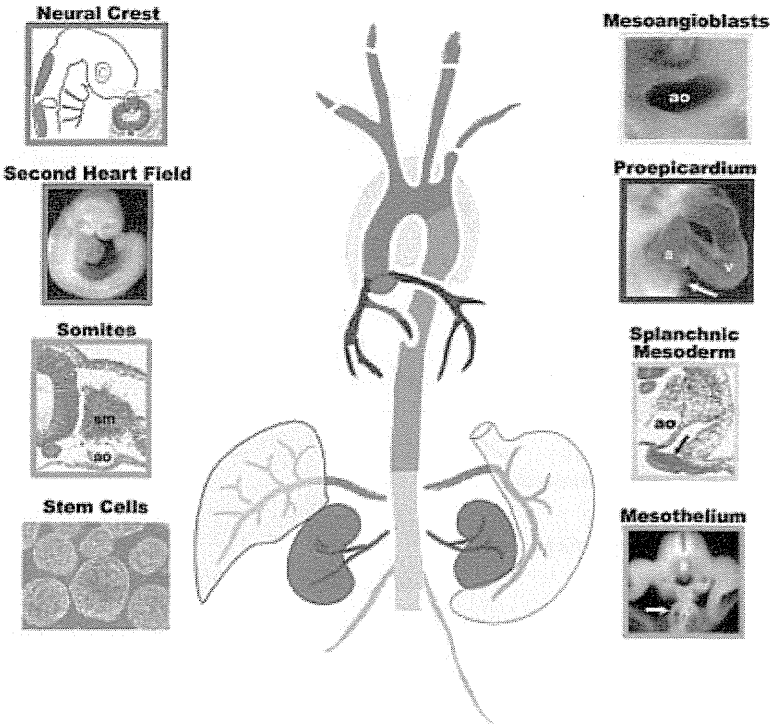
Neural Crest
Second Heart Field
Somites
sm
ao
Stem Cells
Mesoangioblasts
ao
Proepicardium
Splanchnic Mesoderm
ao
Mesothelium

Fig.4

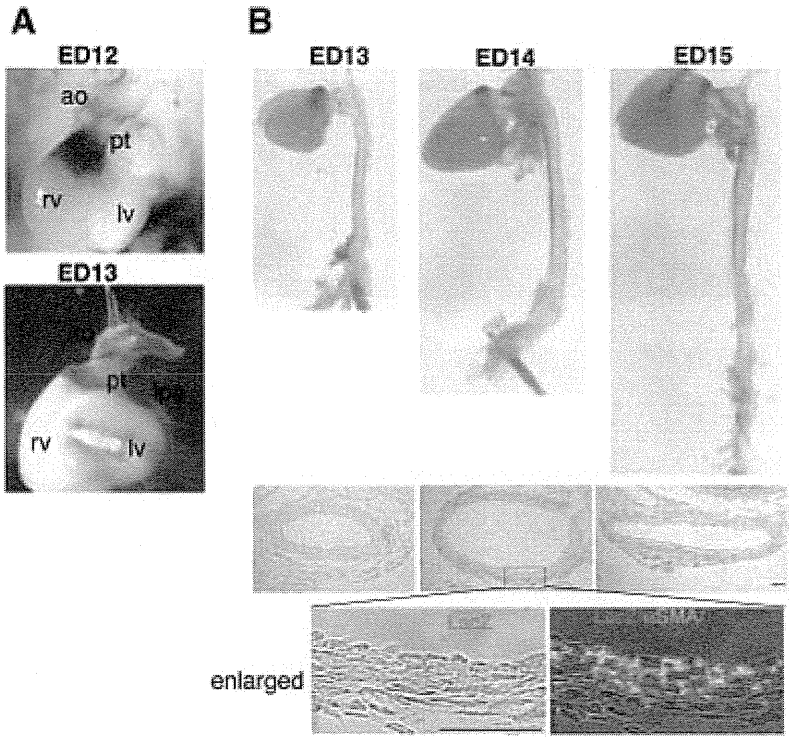

Fig.5

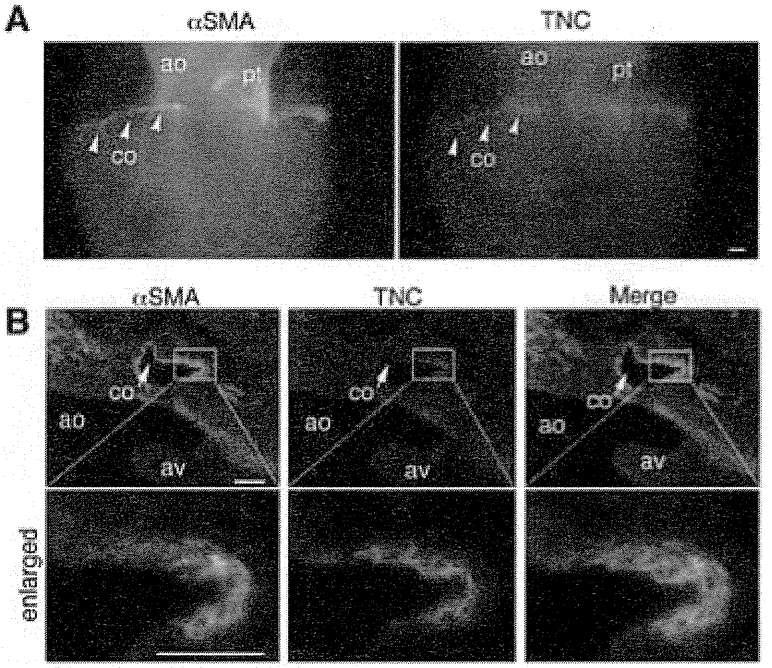

Fig.6

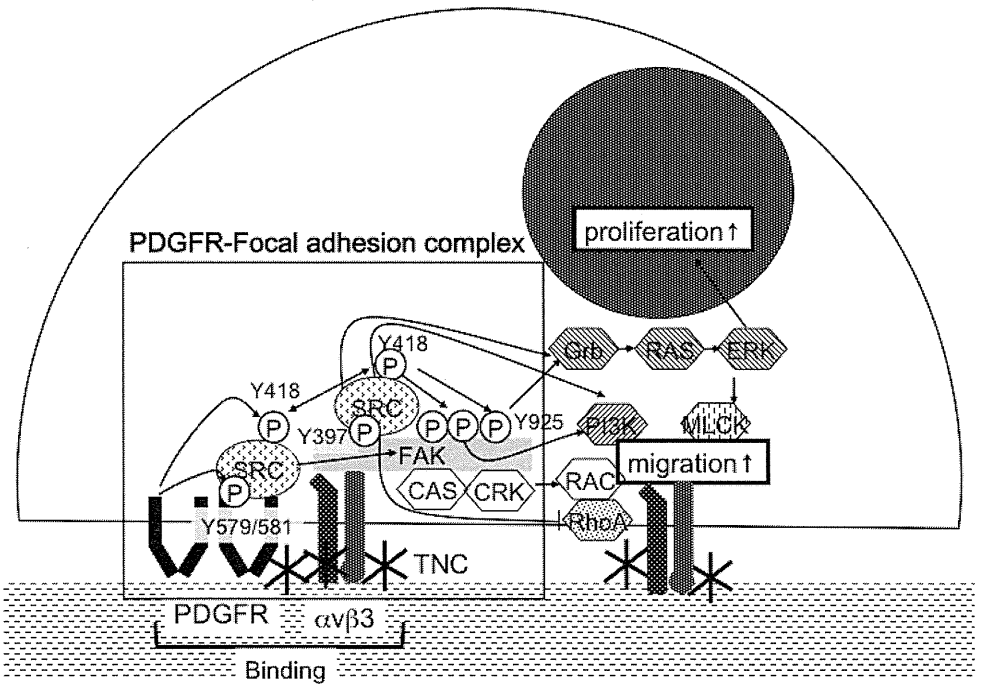
PDGFR-Focal adhesion complex
proliferation↑
Grb
RAS
ERK
Y418
Y418
SRC
Y397
Y925
PI3K
MLCK
SRC
FAK
migration↑
CAS
CRK
RAC
RhoA
Y579/581
TNC
PDGFR
αvβ3
Binding

SCIENTIFIC REPORTS

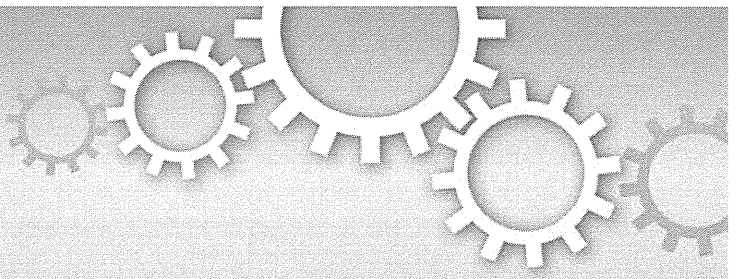

OPEN

SUBJECT AREAS:
SIGNAL TRANSDUCTION
MECHANISMS OF DISEASE
EXTRACELLULAR SIGNALLING MOLECULES
ACUTE INFLAMMATION

Received
1 July 2013

Accepted
20 January 2014

Published
11 February 2014

Correspondence and requests for materials should be addressed to H.A. (haoki@med.kurume-u.ac.jp)

Tenascin C protects aorta from acute dissection in mice

Taizo Kimura[1,2,3], Kozoh Shiraishi[2], Aya Furusho[4], Sohei Ito[4], Saki Hirakata[4], Norifumi Nishida[4], Koichi Yoshimura[1,5], Kyoko Imanaka-Yoshida[6,7], Toshimichi Yoshida[6,7], Yasuhiro Ikeda[1,2], Takanobu Miyamoto[4], Takafumi Ueno[4], Kimikazu Hamano[5], Michiaki Hiroe[8], Kazutaka Aonuma[3], Masunori Matsuzaki[1,2], Tsutomu Imaizumi[4] & Hiroki Aoki[1,4]

[1]Department of Molecular Cardiovascular Biology, Yamaguchi University School of Medicine, [2]Division of Cardiology, Department of Medicine and Clinical Science, Yamaguchi University Graduate School of Medicine, [3]Division of Cardiovascular Medicine, Medical Science for Control of Pathological Processes, Graduate School of Comprehensive Human Science, University of Tsukuba, [4]Cardiovascular Research Institute, Kurume University, [5]Department of Surgery and Clinical Science, Yamaguchi University Graduate School of Medicine, [6]Department of Pathology and Matrix Biology, Mie University Graduate School of Medicine, [7]Mie University Research Center for Matrix Biology, Mie University Graduate School of Medicine, [8]National Center for Global Health and Medicine, Tokyo, Japan.

Acute aortic dissection (AAD) is caused by the disruption of intimomedial layer of the aortic walls, which is immediately life-threatening. Although recent studies indicate the importance of proinflammatory response in pathogenesis of AAD, the mechanism to keep the destructive inflammatory response in check is unknown. Here, we report that induction of tenascin-C (TNC) is a stress-evoked protective mechanism against the acute hemodynamic and humoral stress in aorta. Periaortic application of $CaCl_2$ caused stiffening of abdominal aorta, which augmented the hemodynamic stress and TNC induction in suprarenal aorta by angiotensin II infusion. Deletion of *Tnc* gene rendered mice susceptible to AAD development upon the aortic stress, which was accompanied by impaired TGFβ signaling, insufficient induction of extracellular matrix proteins and exaggerated proinflammatory response. Thus, TNC works as a stress-evoked molecular damper to maintain the aortic integrity under the acute stress.

Acute aortic dissection (AAD) is an abrupt destruction of aortic walls that is immediately life-threatening and is more prevalent than the rupture of abdominal aortic aneurysm (AAA), another life-threatening aortic disease in adult[1]. Although AAD imposes a significant health problem, its molecular pathogenesis is largely unknown except for genetic connective tissue diseases, including Marfan syndrome and Loeys-Dietz syndrome[2], which account for approximately 10% of all AAD cases[1].

Multiple lines of evidence indicates the central role of inflammation in aortic pathology associated with the connective tissue diseases[2]. In these diseases, affected aortic tissue manifests histological abnormalities, including degeneration of extracellular matrix (ECM) and cellular infiltration, which indicate that chronic inflammation precedes the aortic dissection and rupture. As for the animal model of AAD, pathological stress by angiotensin II (AngII) infusion to aged mice induces AAD in an IL-6/MCP-1-dependent manner, underscoring the importance of the proinflammatory response[3]. However, common form of human AAD is characterized by the disruption of the intimomedial layer of aortic walls that otherwise show minimal histological abnormalities[1], suggesting that chronic inflammation alone may not explain the pathogenesis of common AAD.

Although hypertension is a known risk for human AAD, high blood pressure alone does not result in the destructive inflammatory response of aorta in most people. Likewise, AngII infusion into young mice does not cause AAD or other destructive inflammatory response[4]. These facts suggest the presence of a protective mechanism to keep the destructive inflammatory response in check to maintain the integrity of the aortic walls under the stress. Although such a protective mechanism of aortic walls, if exists, may be involved in pathogenesis of AAD, its molecular nature is unknown.

During the investigation into the role of a matricellular protein tenascin C (TNC) in AAA pathogenesis[5], we serendipitously discovered that TNC is involved in pathogenesis of AAD, but not in that of AAA, subsequent to combined insults with periaortic $CaCl_2$ (Ca) treatment[6,7] and AngII infusion. Ca treatment caused stiffening of aorta, a known risk factor for AAD in humans, and augmented the hemodynamic stress and TNC expression by AngII in the aorta. In turn, TNC expression was essential for reinforcing the tissue by the expression of ECM

proteins and for ameliorating an excessive proinflammatory response both in aortic tissue *in vivo* and in aortic smooth muscle cells *in vitro*. Our findings indicate that stress-induced TNC expression is a previously unrecognized protective mechanism in aortic walls, of which failure leads to AAD development.

Results

Development of AAD in TNC-deficient mice. We first investigated the role of TNC in a mouse model of AAA by Ca treatment of the infrarenal aorta[6,7], as we recently found that TNC expression is associated with inflammation and tissue destruction in AAA[5]. However, Ca treatment caused comparable AAA in wild type (WT) and *Tnc*-null (TNC-KO) mice (Supplementary Figs. 1a and 1b) 6 weeks after the Ca treatment when this model reaches the plateau of AAA growth[7], indicating that TNC did not play a major role in the chronic tissue destruction in this AAA model. We then treated mice with AngII infusion (1,000 ng/min/kg) in addition to Ca (Ca + AngII) to further stress the aortic walls. Ca + AngII caused comparable increase in the systolic blood pressure in WT and TNC-KO mice (Supplementary Fig. 1c). Again, Ca-treated aorta segments from WT and TNC-KO mice showed comparable AAA (Fig. 1a, brackets, Supplementary Fig. 1a, b). Unexpectedly, five of 15 TNC-KO mice showed a striking enlargement of the suprarenal aorta after Ca + AngII (Fig. 1a, arrowheads), even though this part of aorta was not exposed to Ca treatment. An additional two TNC-KO mice died of suprarenal aortic rupture. Thus, nearly half of the TNC-KO mice developed suprarenal aortic lesions, whereas WT mice showed no such lesions ($P < 0.01$ compared to WT, Fig. 1b). Although AngII alone caused enlargement of the suprarenal aorta in two TNC-KO mice, the incidence was significantly lower than in Ca + AngII mice ($P < 0.05$).

To better understand the nature of the lesions, we observed the enlarged suprarenal aortae in TNC-KO mice by optical coherence tomography (OCT). The OCT images revealed the "double-barrel" appearance of the true and false lumens that were connected by a narrow channel (Fig. 1c, d, Supplementary Movies 1 and 2), which is a typical finding in human AAD. Ultrasonography of live mice (Supplementary Fig. 2a) also showed the true and false lumens. Histological study demonstrated that the structure of intimomedial layer of the true lumen was largely preserved, but there was an disruption of the medial layer, a hallmark of AAD, in the transition to the fibrous wall of the false lumen (Fig. 1e, Supplementary Fig. 2b). Whereas the intimomedial disruption in human AAD is followed by the longitudinal tearing of the medial layer, the aortic lesions in mice mainly manifested the rupture of aorta and formation of pseudoaneurysm, probably because the medial layer consists of about 100 elastic lamellae in human but only 3–4 elastic lamellae in mice. From these findings we concluded that TNC-KO developed AAD, which recapitulate the intimomedial disruption as observed in human AAD, upon the Ca + AngII treatment.

Synergistic augmentation of hemodynamic stress and TNC expression by Ca + AngII. Although others reported that AngII infusion (2,500 ng/min/kg) causes AAD in old mice (7–12 months old)[3], AngII (1,000 ng/min/kg) alone in younger WT mice (10–14 weeks of age) did not induce an obvious AAD in our hands (Fig. 1a, b). This raises two questions: (1) Why does infrarenal Ca treatment influence AAD development in the distant suprarenal aorta in TNC-KO mice? (2) How is TNC involved in AAD pathogenesis? Aortae with AAD showed an intact segment (Fig. 1a, double arrow) between the Ca-treated segment (Fig. 1a, bracket) and AAD (Fig. 1a, arrowheads), suggesting that direct propagation of Ca-induced tissue destruction was unlikely to have caused suprarenal AAD. Serum cytokine levels in WT mice showed no significant changes 6 weeks after the AngII or Ca + AngII treatment (Supplementary Fig. 3), indicating an absence of generalized inflammation in this setting.

We reasoned that Ca treatment might cause aortic stiffening, a known risk factor for AAD in humans[8,9], by inducing periaortic fibrosis and loss of the spring-like elastic lamellae structures (Fig. 2a, b and Supplementary Fig. 1a). The stiffening of the infrarenal aorta would then augment the hemodynamic stress on the suprarenal aorta due to the loss of the Windkessel effect[10]. Indeed, the pressure-diameter (PD) curve of excised aortae after Ca + AngII treatment showed a marked downward shift, indicating stiffening in the infrarenal aorta, whereas that of the suprarenal aorta showed no change (Fig. 2c). Hemodynamic measurements by aortic catheterization in live mice indicated that one week of Ca + AngII treatment increased dP/dt (Fig. 2d) at comparable blood pressures (Supplementary Fig. 4a). Ultrasonography performed in live 1 week after the Ca + AngII treatment revealed a reduction in the systolic descent rate of the infrarenal aorta and an augmentation of that of the suprarenal aorta (Supplementary Fig. 4b).

As *Tnc* is a mechanosensitive gene[11,12], we examined its expression using the *Tnc* reporter mice in which *lacZ* was knocked into one of the *Tnc* loci[13]. In control mice without Ca or AngII treatment, *Tnc* expression was restricted to the lower aorta (Fig. 2e, Supplementary Fig. 5a) where dP/dt was higher than the upper aorta (Fig. 2d). Infrarenal Ca treatment induced *Tnc* expression in the infrarenal aorta[5], and systemic AngII infusion resulted in *Tnc* expression in the entire aorta (Supplementary Fig. 5a). Ca and AngII treatments synergistically enhanced and prolonged *Tnc* expression in the upper aorta (Fig. 2e, Supplementary Fig. 5a), probably due to the augmented hemodynamic stress (Fig. 2d). Histological analysis revealed that TNC was expressed by the smooth muscle α-actin positive cells, most likely smooth muscle cells, in the medial layer (Supplementary Fig. 5b). The synergy of Ca and AngII in enhancing *Tnc* gene expression was reflected in the increase in serum TNC levels 6 weeks after the treatment of WT mice (Supplementary Fig. 5c). Therefore, Ca treatment caused the stiffening of the infrarenal aorta and augmented AngII-induced hemodynamic stress and *Tnc* expression.

Transcriptome analysis before AAD development. We next investigated how TNC was involved in the pathogenesis of AAD. Serial ultrasonography in TNC-KO mice revealed that AAD developed after 10–15 days of Ca + AngII treatment. We performed a transcriptome analysis 1 week after starting Ca + AngII in the suprarenal aorta; at this time, there was no obvious AAD. The Ca + AngII-induced genes comprised 1,115 probe sets with z scores > 2 in either WT or TNC-KO mice. Analysis using Database for Annotation, Visualization and Integrated Discovery (DAVID)[14] identified a functional annotation cluster with the highest enrichment score (28.54) with the gene ontology terms "extracellular region," "extracellular region part" and "extracellular space," which contained 182 probe sets (Fig. 3). Hierarchical average linkage clustering of these probe sets revealed distinct subclusters. Subcluster #1, which was induced strongly in WT mice but weakly in TNC-KO mice, contained genes encoding ECM proteins, including elastin, collagens, fibrillin-1 and fibulins, which are essential for aortic tissue integrity[2,15]. Subcluster #2, induced weakly in WT mice but strongly in TNC-KO mice, contained genes encoding proinflammatory cytokines and chemokines, which are reportedly involved in pathogenesis of mouse AAD[3]. Other functional annotation clusters also indicated an ineffective induction of ECM genes and an exaggerated proinflammatory response in TNC-KO mice (Supplementary Fig. 6a–d).

Mechanism of TNC-mediated aortic protection. We confirmed the exaggerated proinflammatory response by quantitative RT-PCR in the suprarenal aorta of TNC-KO mice 1 week after the Ca + AngII treatment (Fig. 4a, Supplementary Fig. 7a). As TNC is expressed in medial smooth muscle cells (Supplementary Fig. 5b), we examined the TNC in aortic smooth muscle cells in culture. We cultured suprarenal aortic smooth muscle cells from TNC-KO mice in the

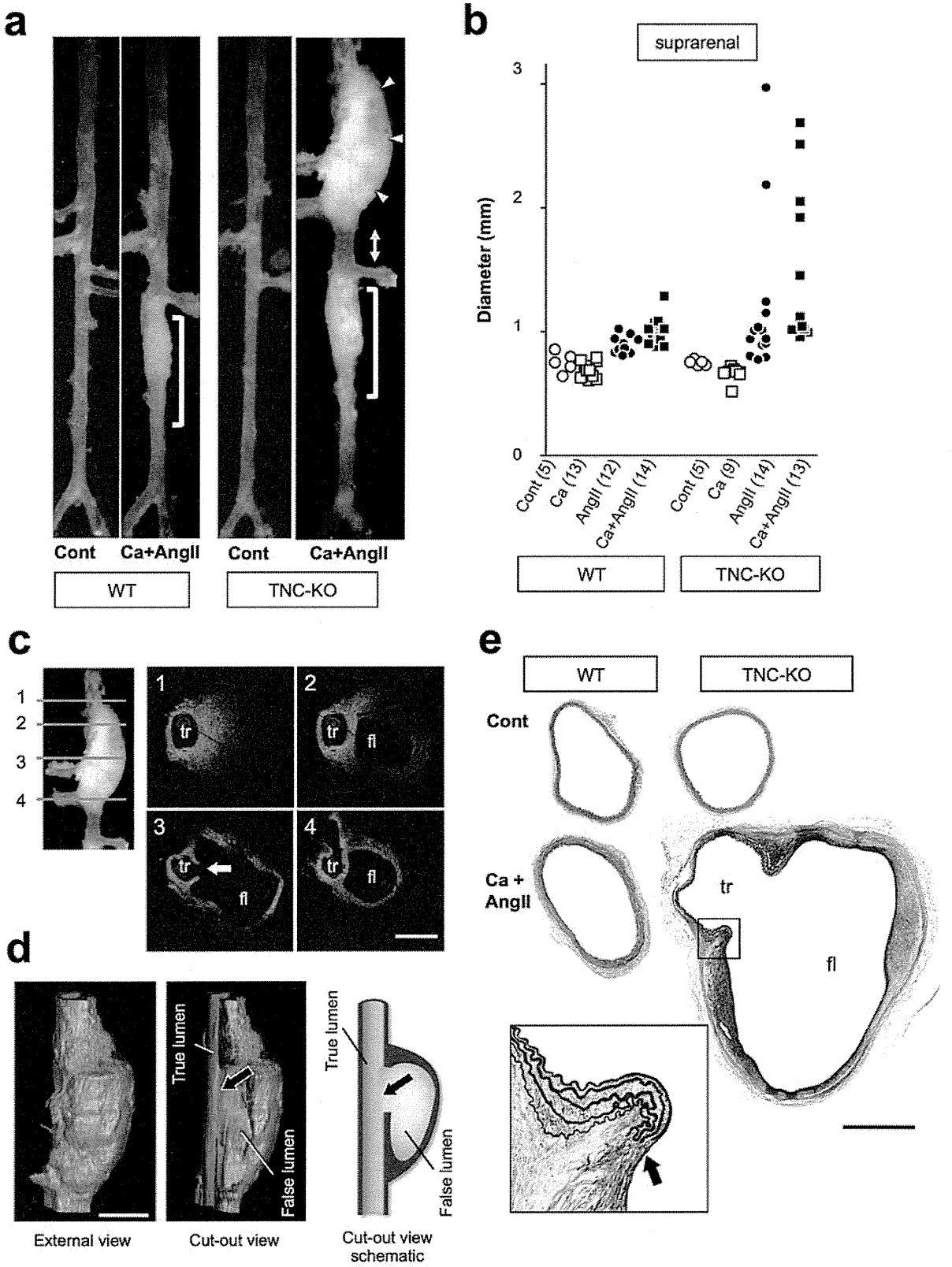

Figure 1 | Aortic dissection elicited by Ca + AngII treatment in TNC-KO mice. (a) Representative images of aortae from WT and TNC-KO mice. Brackets indicate the Ca-treated segments. Arrowheads and a double arrow indicate the enlarged and normal segment of the TNC-KO aorta, respectively. (b) Diameters of suprarenal aortae from WT or TNC-KO mice with the indicated treatment. Animal numbers are indicated in parentheses. (c), (d) Representative images of optical sections (c) and 3D reconstruction (d) by optical coherence tomography of an enlarged TNC-KO aorta. Arrows indicate the dissection of the aortic wall. (e) Elastica van Gieson (EVG) staining of suprarenal aortae from WT and TNC-KO mice. The inset shows an enlarged image of the area in the square. The arrow points to the disrupted medial layer. True (tr) and false (fl) lumens of the aorta are indicated. Bars, 0.5 mm.

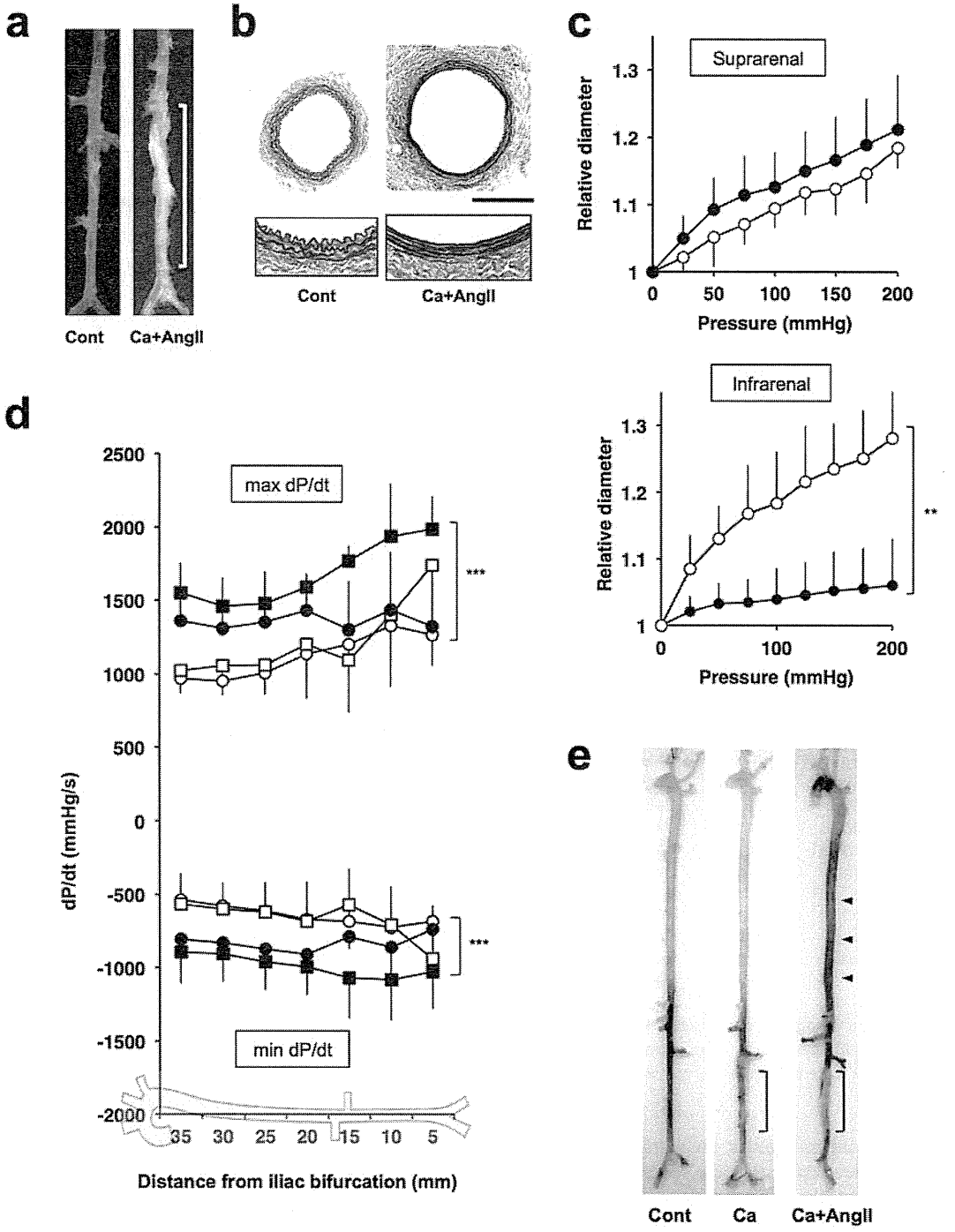

Figure 2 | Aortic stress elicited by Ca + AngII treatment. Representative photographs (a) and EVG staining (b) of infrarenal aortae without (Cont) and with Ca + AngII treatment. The bracket indicates the Ca-treated region. Bar, 0.5 mm. (c) Pressure-diameter (PD) curves of the suprarenal (upper panel) and the infrarenal (lower panel) regions of the aortae are shown for untreated controls (open circles) and 6 weeks after Ca + AngII treatment (closed circles). Data, which are expressed relative to the aortic diameter at 0 mmHg, are the mean ± standard deviation (SD) of four independent observations for each group. (d) Maximum and minimum dP/dt of the pressure wave is shown for control (open circles), Ca treatment (open squares), AngII treatment (closed circles) and Ca + AngII treatment (closed squares) after 1 week of treatment at various positions in the aortae, as illustrated at the bottom of the panel. Data are the mean ± SD of eight independent observations. $^{**}P < 0.01$ and $^{***}P < 0.001$ compared to control. (e) β-galactosidase staining of *Tnc* reporter mice aortae with or without 6 weeks of Ca + AngII treatment. Brackets indicate the Ca-treated segment. Arrowheads indicate enhanced β-galactosidase activity.

presence or absence of exogenous TNC and then stimulated them with TNFα to investigate the cellular response to the proinflammatory environment. Quantitative RT-PCR revealed that a higher proinflammatory response was elicited by TNFα in the absence of exogenous TNC (Fig. 4b, Supplementary Fig. 7b). TNFα also suppressed many of the collagen family genes[16], which was partially prevented by exogenous TNC (Supplementary Fig. 7c), suggesting that the presence of TNC supported the expression of the collagen family genes. Therefore, deletion of *Tnc* resulted in the exaggerated the proinflammatory response and the ineffective induction of ECM genes in aortic tissue *in vivo* and in aortic smooth muscle cells *in vitro*.

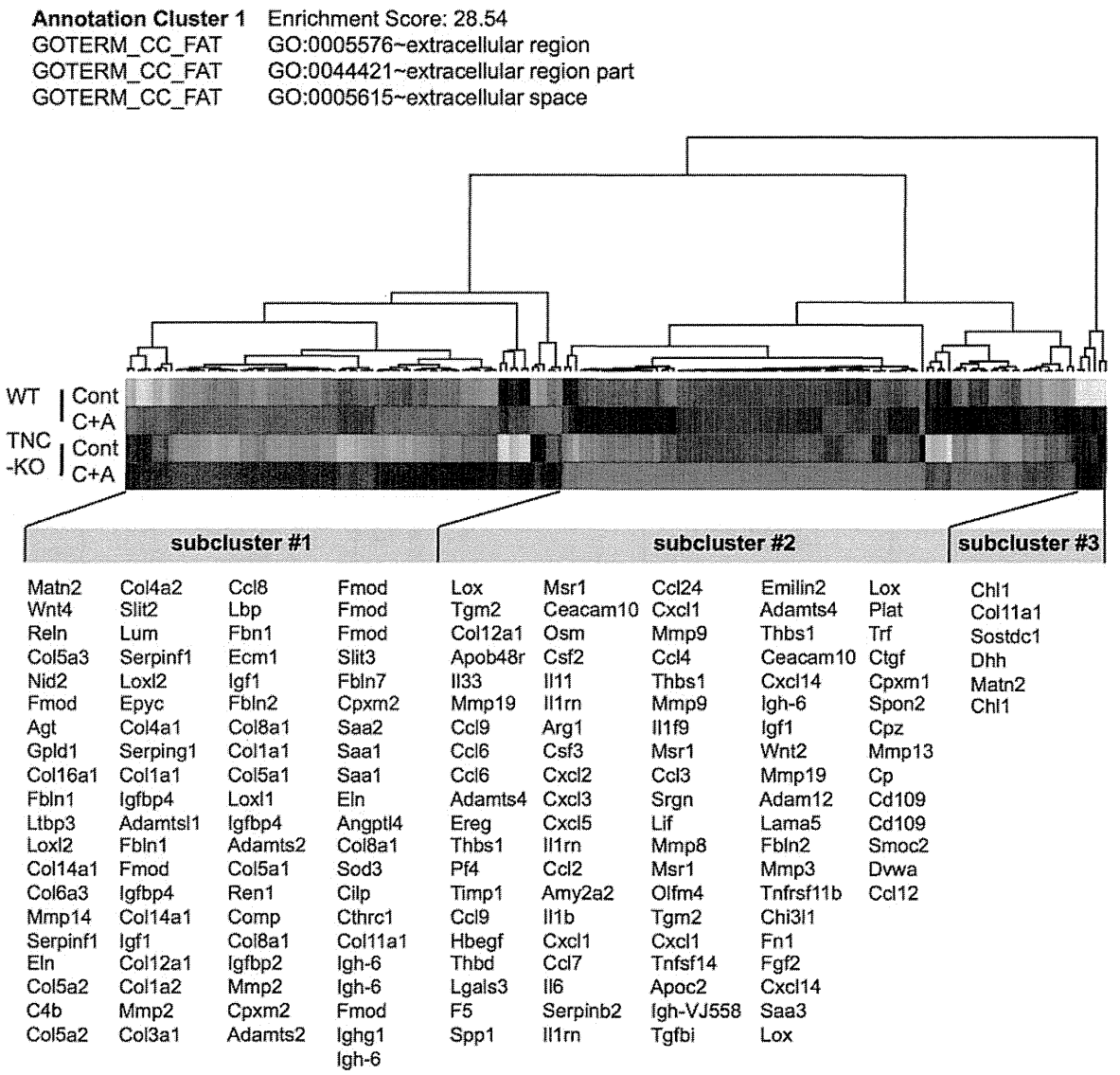

Figure 3 | Transcriptome of the mouse aorta before dissection. Heat map diagram of average linkage hierarchical clustering of the genes induced by Ca + AngII in WT and in TNC-KO mice. The functional annotation cluster is shown with the highest enrichment score by DAVID analysis. RNA samples were from WT or TNC-KO mice with (C + A, n = 8) or without (Cont, n = 5) Ca + AngII treatment for 1 week.

Induction of proinflammatory genes, including IL-6 and CCL-2 (MCP-1), before AAD development is consistent with a previous report[3]. On the other hand, the impact of the suppression of ECM genes in this experimental setting was to be investigated. Picrosirius red staining of the suprarenal aorta revealed that medial collagen deposition did not differ between untreated WT and TNC-KO mice (Fig. 4c, Supplementary Figs. 8a and 8b), consistent with the notion that TNC is dispensable for the normal development[13]. While 1 week of Ca + AngII treatment was associated with an increase in medial collagen deposition in WT mice, the response was weaker in TNC-KO mice (Fig. 4c). Obvious changes in adventitial sirius red staining was not observed (Supplementary Fig. 8b), possibly because collagen was already abundant in samples without Ca + AngII treatment. The increase in medial collagen deposition in WT by Ca + AngII treatment was accompanied by the increase in the immunoreactivity of type I collagen (Fig. 4d, Supplementary Fig. 8c). Immunoreactivity of lysyl oxidase, a cross-linking enzyme for collagen and elastin, showed a decrease by Ca + AngII treatment whereas that of fibronectin showed no obvious change (Supplementary Fig. 8c), although the expressions of their genes were increased by Ca + AngII treatment (Fig. 3). This may be due to the post translational regulation of protein levels as recently reported for lysyl oxidase[17].

The PD curve of the suprarenal aorta from untreated TNC-KO mice overlapped with that of WT mice (Fig. 4e), indicating that TNC is dispensable for the normal biomechanics of the aorta. The PD curve 1 week after the Ca + AngII treatment showed a mild but significant ($P < 0.05$) upward shift in WT mice. In TNC-KO mice, Ca + AngII treatment caused a more prominent upward shift of the PD curve ($P < 0.001$ compared with WT control), suggesting a greater loss of wall strength than in WT mice. Notably, the PD curve of the Ca + AngII-treated WT suprarenal aortae at 6 weeks returned to that of the untreated control, suggesting a recovery of once-lost wall strength.

Cellular response in aorta before AAD development. To better understand the cellular responses in the aorta before the AAD development, we took advantage of the imaging cytometry that can analyze the intracellular signal response at the single cell levels in the context of the aortic tissue. We obtained suprarenal aortic tissue from WT or TNC-KO mice 1 week after the Ca + AngII

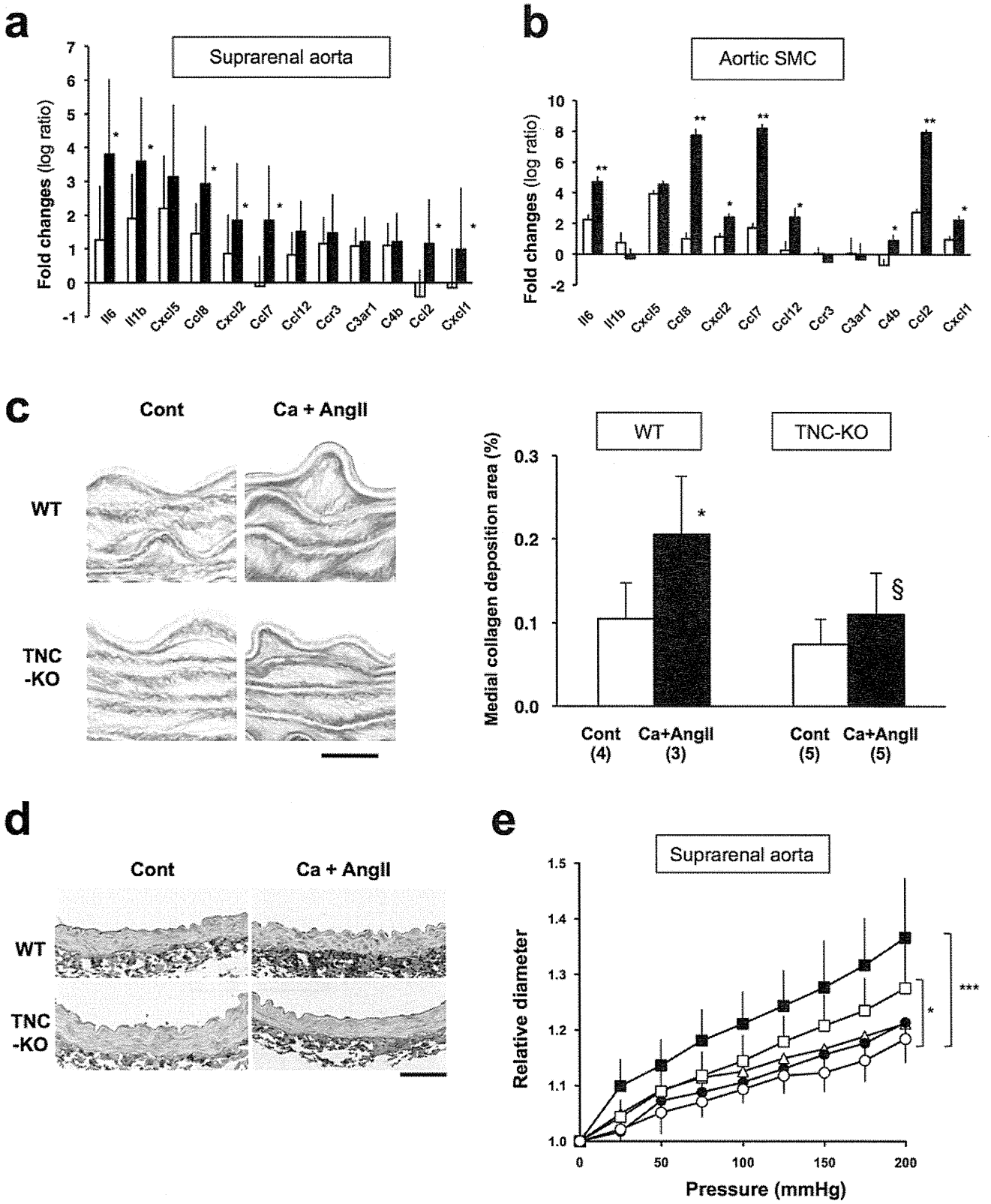

Figure 4 | Stress response of the mouse aorta before dissection. (a) Fold induction of proinflammatory genes in the suprarenal aorta of WT (open columns) or TNC-KO mice (closed columns) after 1 week of Ca + AngII treatment. Shown are the 12 genes with the highest induction in TNC-KO aortae out of 84 proinflammatory genes using a commercially available PCR array. (b) Genes induced by 10 ng/mL TNFα in TNC-KO aortic smooth muscle cell (SMC) culture in the presence (white) or absence (black) of exogenous TNC (10 μg/mL). Data are the mean ± SD of eight independent observations. *P < 0.05 and **P < 0.01 compared to those with TNC. (c) Picrosirius red-stained medial layer of suprarenal aorta in WT and TNC-KO mice with or without Ca + AngII treatment for 1 week. Bar, 10 μm. Data are the mean ± SD of five independent observations. *P < 0.05 compared to WT control. §P < 0.05 compared to WT Ca + AngII. (d) Representative images of type I collagen immunostaining are shown for WT and TNC-KO aortae with or without 1 week of Ca + AngII treatment. Bar, 50 μm. (e) PD curves of the suprarenal regions of the excised aortae from WT (open symbols) and TNC-KO (closed symbols) mice treated with (squares) or without (circles) Ca + AngII for 1 week. Open triangles indicate WT with Ca + AngII for 6 weeks. Data are the mean ± SD of seven independent observations. *P < 0.05 and ***P < 0.001 compared to WT control.

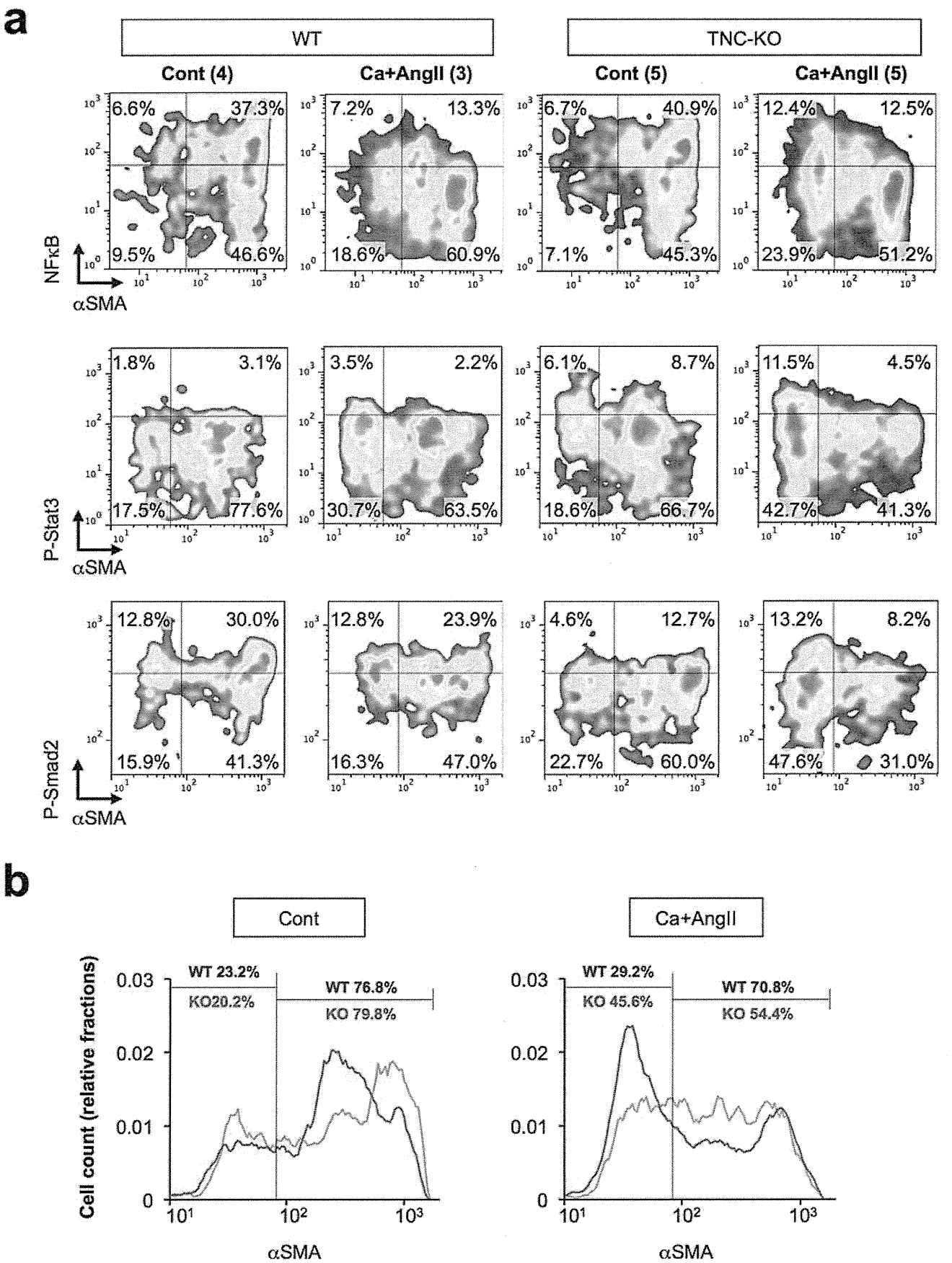

Figure 5 | Cellular responses in mouse aorta before AAD development. (a) Imaging cytometric analyses of aortae. Scattergrams are shown for the fluorescence intensities of NFκB, phospho-Stat3 (P-Stat3) and phospho-Smad2 (P-Smad2) immunostainings, along with that of smooth muscle α-actin (αSMA). Aortae were obtained from WT or TNC-KO mice with or without 1 week of Ca + AngII treatment. Animal numbers are indicated in parentheses. (b) Analyses of αSMA intensities. Blue and red lines indicate the histograms of WT and TNC-KO (KO), respectively.